NANO: Brief Reports and Reviews
Vol. 8, No. 3 (2013) 1350031 (8 pages)

DOI: 10.1142/S1793292013500318

World Scientific
www.worldscientific.com

EVALUATION OF THE ANTITUMOR ACTIVITY BY CdTe QDs WITH VERBASCOSIDE

XIAO-HUI ZHAO[*,†,‡,§] and HUI-LAN YUE[*,¶]
[*]*Key Laboratory of Adaptation and Evolution of Plateau Biota*
Northwest Plateau Institute of Biology
Chinese Academy of Sciences
Xining 810001, P. R. China

[†]*State Key Laboratory Breeding Base-Key*
Laboratory for Plateau Crop Germplasm Innovation
and Utilization of Qinghai Province, Xining 810016, P. R. China

[‡]*Graduate University of Chinese Academy of Sciences*
Beijing 100049, P. R. China
[§]*xhzhao@nwipb.ac.cn*
[¶]*hiyuehlx@163.com*

PING LI[‖] and XIN ZENG[**,††]
State Key Laboratory of Reproductive Medicine
Department of Gynecological Endocrine
Nanjing Maternity and Child Health Care
Hospital Affiliated to Nanjing Medical University
Nanjing 210029, P. R. China
[‖]*liping0099@126.com*
[**]*august555482@hotmail.com*

GEN ZHANG[††]
Department of Cell Biology
School of Basic Medical Sciences
NanJing Medical University
Nanjing 210029, P. R. China
zhanggen123@126.com

Received 19 October 2012
Accepted 4 March 2013
Published 19 April 2013

Cadmium telluride quantum dots (QDs) have received significant attention in biomedical research because of their potential in drug delivery. In this study, the chemotherapeutic agent Verbascoside (VB) was immobilized successfully onto CdTe QDs by covalent bonding between the −OH group of VB and the −COOH group of CdTe QDs. The amount of VB that could be immobilized depended on the concentration of −COOH groups (succinic acid) on the

[††]Corresponding authors.

surface of the CdTe QDs. Apoptotic staining, DNA fragmentation and flow cytometry analysis further demonstrated that compared with CdTe QDs or VB treatment alone, the apoptosis rate increased after the treatment of CdTe QDs together with VB (VB−QDs) in HepG2/ADM cells. We observed that VB−QDs treatment could clearly activate apoptosis-related Caspase 3 expression in HepG2/ADM cells. Moreover, our *in vivo* study indicated that the treatment of VB−QDs effectively inhibited the human hepatoma HepG2/ADM nude mice tumor growth. The increased cell apoptosis rate was closely correlated with the enhanced inhibition of tumor growth in the studied animals. Thus, VB−QDs may serve as a possible alternative for therapeutic approaches for some cancer treatments. In summary, studies have shown that cancer cells are treated by the presence of VB−QDs nanoparticles based on analysis of cell apoptosis.

Keywords: Quantum dots; apoptosis; caspase 3; verbascoside.

1. Introduction

Cancer is becoming the leading cause of death worldwide.[1] Multidrug resistance, a phenomenon of resistance of cancer cells to structurally diverse and mechanically unrelated anti-cancer drugs, is a major obstacle to successful cancer chemotherapy.[2] Current treatment of cancer with chemotherapy is insufficient in selectivity, thus induces toxicity to normal cells. This fact accentuates the need for a new generation of more effective therapies for cancer.

Previous phytochemical studies have demonstrated that flavonoids and phenylpropanoid glycosides were the major bioactive constituents of herb Tsoong plant (Chinese name, Banchunmaxianhao, BCM).[3] Among these constituents, VB [see Fig. 2(A)] has attracted a great deal of attention due to their pharmacological properties; these properties include hepatoprotective, anti-inflammatory, antitumor, cytotoxic, antioxidant activities and so on. Verbasco side (VB) has been isolated and purified by high-performance liquid chromatography (HPLC) and column chromatography from BCM.

Nanomaterials have dimensional analogies similar to physiological molecules such as proteins and nucleic acids and therefore have been exploited in various biomedical applications, such as tissue engineering, biosensing, medical diagnostics and therapeutics.[4] Nanoparticles have been proposed as diagnostic, therapeutic and theranostic agents for a wide variety of human diseases. Quantum dots (QDs) are fluorescent nanoparticles of semiconductor material with unique photophysical properties that give them significant advantages over organic dyes and proteins commonly used in biomedical imaging.[5] As a material with great potential for a variety of practical applications, CdTe QDs have also always received great concern due to their drug delivery for biomedical applications.

In this study, we have developed a procedure employing highly luminescent and stable CdTe core/shell QDs for VB intracellular delivery and killing effect in cancer therapy during long term. The positively charged VB molecule OH group successfully linked with surface of carboxylic group of CdTe QDs (i.e., capped with succinic acid) enhance drug uptake via EDC coupling method. We also report VB−QDs treating adriamycin-resistant human hepatoma HepG2 cells, as well as nude mice as model animal systems. We found that VB−QDs greatly increased the apoptosis against cancer cells. The *in vivo* study also revealed that VB−QDs showed a good activity to inhibit tumor growth.

2. Materials and Methods

2.1. *Materials*

BCM were collected from Gangcha, QingHai, China and identified by Prof. Li-Juan Mei (Northwest Institute of Plateau Biology, Chinese Academy of Sciences). Materials used for HPLC analysis was of analytical grade.

2.2. *Extract VB from BCM plant*

BCM (500 g) were powdered, and extracted three times with 70% EtOH under reflux. After concentration under vacuum, the residues were suspended in distilled water and extracted with light petroleum, EtOAc and *n*-butanol, respectively. The *n*-butanol solutions were evaporated to dryness under vacuum at 70°C to generate *n*-butanol extract, which was loaded on silica gel column and eluted with various

proportions of a mixture of chloroform−methanol. The chloroform−methanol (3:1) fraction was concentrated to produce crude sample for subsequent high-speed counter-current chromatography (HSCCC) isolation and purification. With a two-phase solvent system composed of chloroform−*n*-butanol−methanol−water (4:3:4:5, v/v), the crude sample was separated to yield VB. Its chemical structure was identified by ^{1}H NMR, and ^{13}C NMR.[6]

2.3. *Preparation of drug-coated QDs*

The mixture was stirred at room temperature with nitrogen. Approximately 2 mg of the VB was pooled with the 30 mg QDs solution with EDC overnight. The final product was separated from the solution centrifuged at 10 000 rpm during 20 min and washed 3 times and then resuspended in 300 mL distilled H_2O. The VB−QDs were observed under the transmission electron microscopy (TEM) and dynamic light scattering (DLS) measurement was carried out (ELS- 8000L, Japan).

2.4. *Fourier Transform Infrared Spectroscopy (FTIR)*

Absorption of VB on the surface of QDs was examined by a Nicolet Avatar 360 FT-IR spectroscopy. Pellets for FT-IR analysis were prepared by mixing the lyophilized samples of VB−QDs formulations with spectroscopic grade KBr powder.

2.5. *Determination of drug loading*

To determine the amount of VB loading, 1 mg VB−QDs was resolved in 30 mL of DMSO. The samples were centrifuged for 10 min at 16 000 g using Eppendorf microcentrifuge. VB concentration was determined by HPLC technique as described in Sec. 2.2.

2.6. *Cell culture and MTT assay*

HepG2/ADM cells (drug-resistant cell line) were cultured in RPMI 1640 medium supplemented with 10% fetal bovine serum, adriamycin (Sigma, USA) at 37°C in a humidified air-5% CO_2 atmosphere. HepG2/ADM cells were seeded in 96-well tissue culture plates at a density of 5×10^3 cells per well. After 24 h, cells were treated with VB−QDs or VB. The cytotoxicity was evaluated by determining the viability of the HepG2/ADM cells after incubation for 48 h. After MTT solution was added to each well for 4 h, the supernatant was removed and DMSO was added. The optical density (OD) was read at a wavelength of 540 nm. All experiments were performed in triplicates. Relative inhibition of cell growth was expressed as follows: %cell viability = [OD]test/[OD]control × 100%.

2.7. *Apoptosis measurements*

HepG2/ADM cells were stained with acridine orange ethidium bromide (AO/EB) dye mix and viewed using a fluorescence microscope with VB−QDs treatment. The apoptotic cells were detected by Flow Cytometry using Annexin-V-FITC method. In addition, the cells (VB−QDs treatment) were lysed with 100 μL DNA Ladder Extraction Buffer for 1 min. Centrifuge for 10 min at 4500 rpm. DNA ladder were electrophoresed and photographed. Cancer cells lysed in modified RIPA buffer were subjected to immunoblot analysis. Caspase 3 obtained was purchased from the Cell Signaling Technologies (Danvers, MA). Proteins were detected by enhanced chemiluminescence (ECL, Thermo scientific).

2.8. *Scanning electron microscopic observations (SEM) analysis of cancer cells*

HepG2/ADM cells were cultured with VB−QD. After 1 h of incubation, the cells were fixed with 2.5% glutaraldehyde overnight. They were then washed with 30, 50, 70, 80, 90, 95 and 100% ethanol. These cover slips were then carefully dried before SEM experiments.

2.9. *Experimental animals*

The female nude mice (six-week old) were purchased from the Animal Feeding Farm of National Institute for the Control of Pharmaceutical and Biological Products (P. R. China). All HepG2/ADM tumor mice were housed in the animal facility, and animal experiments; (1) Control ($n = 7$); (2) VB ($n = 7$); (3) VB−QDs ($n = 7$) that were conducted followed the guidelines by the Animal Research Ethics Board of NanJing Medical University. Animals were kept in the facility with free access to food and water. Injection was intravenously administered by tail vein at day 0, 2, 4, 6, 8,

10, 12, 14, 16 and 18. The tumor volume of nude mice were measured and calculated at the 20th day after treatment. The tumor volume calculation was performed using the formula $V = \pi/6 \times [(a+b)/2]^3$, where a is the largest and b is the smallest diameter of the tumor.

2.10. *In situ apoptosis by TUNEL staining*

Apoptotic cell death in deparaffinized tumor tissue sections was detected using terminal deoxynucleotidyl transferase-mediated dUTP nick end-labeling (TUNEL) with the Klenow DNA fragmentation detection kit (Roche, USA). Apoptotic cells were identified by the dark brown nuclei observed under a light microscope. A total of 3 slides were generated from each tumor in each group, and then 10 fields from each slide were randomly selected to make the statistical analysis.

3. Results

3.1. *Identification and synthesis of VB structure, and characterization of VB−QDs*

The NMR data of VB was in agreement with published data.[7] VB, yellow needles, 1H NMR spectrum (DMSO, 400 MHz) $\delta = 7.44$ (d,1H, $J = 16.0$ Hz), 7.02 (d,1H, $J = 1.6$ Hz), 6.97 (dd, 1H, $J = 1.6$ Hz, $J = 8.4$ Hz), 6.75 (d,1H, 8.0 Hz), 6.63 (d,1H, $J = 1.6$ Hz), 6.61 (d,1H, $J = 8.0$ Hz), 6.48 (dd,1H, $J = 1.6$ Hz, $J = 8.0$ Hz), 6.19 (d,1H, $J = 16.0$ Hz), 5.00 (s, 1H), 4.70 (t, 1H, $J = 9.2$ Hz), 4.34 (d, 1H, $J = 7.6$ Hz), 3.86 (m, 1H), 3.77 (m, 1H), 3.73 (m, 2H), 3.56 (m, 1H), 3.46 (m, 1H), 3.36 (m, 1H), 3.30 (m, 1H), 3.26 (m, 1H), 3.17 (m, 1H), 3.09 (t, 1H, $J = 9.6$ Hz), 2.67 (m, 2H), 1.02 (d, 3H, $J = 6.0$ Hz). 13C NMR (DMSO, 400 MHz) $\delta = 165.9$, 148.5, 145.8, 145.6, 145.0, 143.6, 129.3, 125.6, 121.7, 119.8, 116.4, 115.9, 115.6, 114.7, 113.7, 102.4, 101.4, 79.2, 74.6, 71.7, 71.6, 70.6, 70.5, 70.4, 69.2, 68.9, 60.8, 35.1, 18.3.

The average diameter of VB−QDs measured by TEM was about 4 nm, as seen in Fig. 1(A). The VB−QDs in cell culture medium were characterized with DLS in Fig. 1(B). The FT-IR spectroscopy proved to be useful to characterize the VB bound onto QDs. The IR peak of C=O (ester) assigned at 1740 cm^{-1} could be seen in VB−QDs as shown in Fig. 1(C). To determine the amount of VB loaded on QDs, we performed HPLC analysis. Results indicated that VB loaded in VB−QDs was 18.3 wt.% (i.e., 183 mg of VB/g of VB−QDs). As shown in Fig. 1(D), the VB−QDs were found to be stable and their optical properties in a sealed bottle remained invariable over one year's storage under ambient condition. Even after the EDC-mediated condensation reaction with VB, the optical properties are still stable.

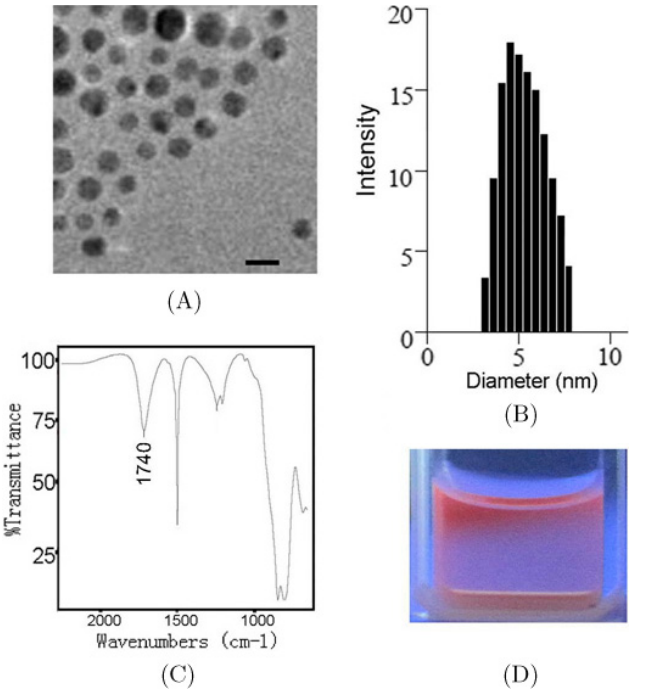

Fig. 1. (A) TEM images of VB−QDs. Bar: 5 nm. (B) The size distribution of VB−QDs in the culture medium characterized by DLS. (C) Analysis of VB−QDs by FT-IR Spectroscopy. (D) The photo of the VB−QDs under an ultraviolet lamp excitation (color online).

3.2. *Cytotoxicity and apoptosis analysis*

In order to examine the acute toxicity of VB, QDs or VB−QDs, HepG2/ADM cells were incubated for 48 h with the treatment in various concentrations as described above. The cell viability, as determined by MTT assay, demonstrates that VB−QDs were toxic in HepG2/ADM cells. Interestingly, as shown in Fig. 2(B), the cell viability decreased profoundly when QDs were loaded with VB, compared with VB or QDs.

The results also demonstrated that the HepG2/ADM cells treated with VB−QDs showed their

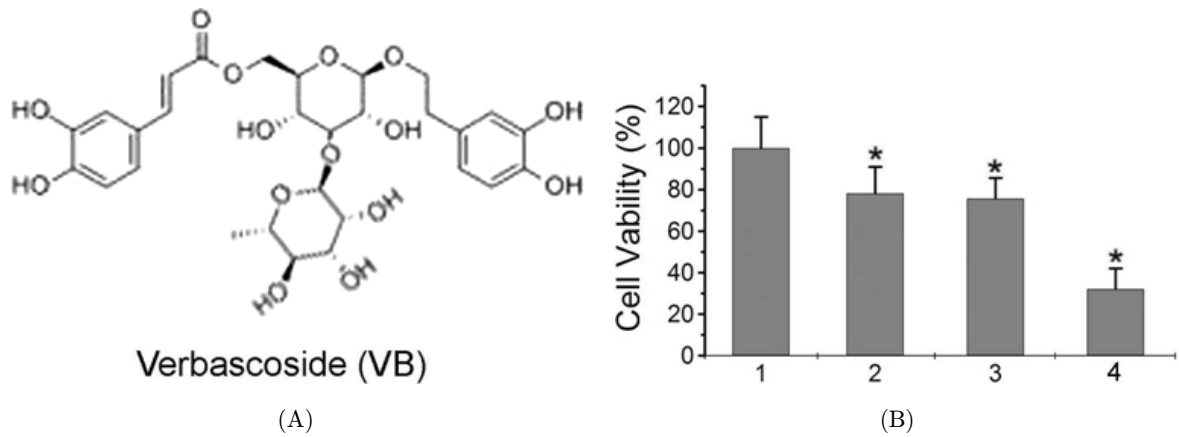

Fig. 2. (A) The chemical structure of VB. (B) Increased growth inhibition induced by VB−QDs treatments in HepG2/ADM cells. HepG2/ADM cells were treated with (1) control treatment, (2) 1.83×10^{-1} mg/L VB, (3) 8.17×10^{-1} mg/L QDs and (4) 1 mg/L VB−QDs, quantitative analysis cells after viability treatments, $^*p < 0.05$, compared to the control treatment.

distinctively marginated and fragmented appearance of apoptosis cells by Acridine Orange/Ethidium Bromide (AO/EB) dye assay. The green apoptotic nuclei were early apoptotic nuclei, and the red apoptotic were late apoptotic nuclei [see Fig. 3(B), a, b]. For the control cells without treatment, cells nuclei were normal [see Fig. 3(B), c, d]. We found that the percentage of apoptotic cells was 65.6%, 34.3% and 11.6% for VB−QDs, VB and control, respectively [see Fig. 3(E)]. Meanwhile, the DNA

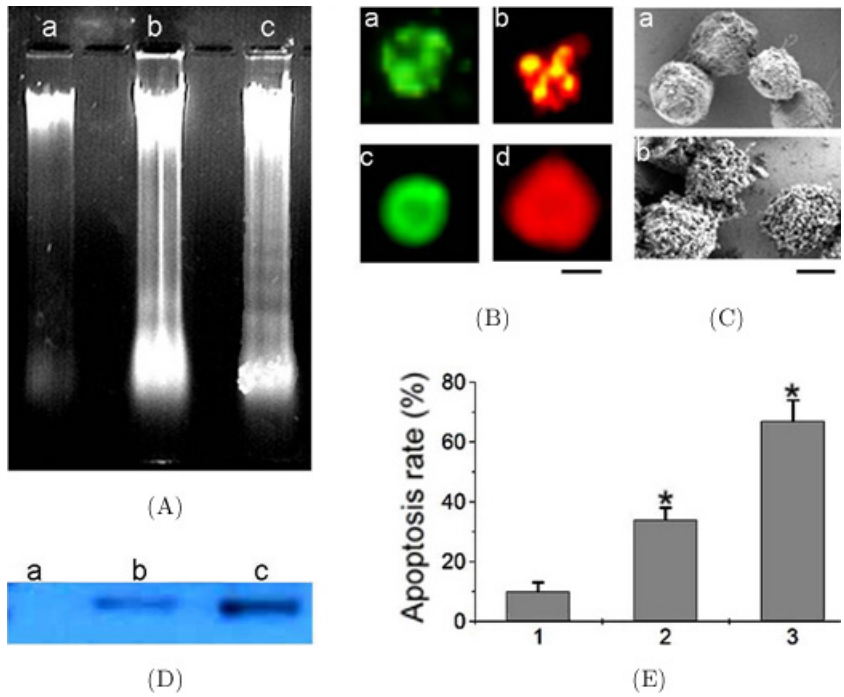

Fig. 3. (A) DNA fragmentation in HepG2/ADM cells after different treatments. HepG2/ADM cells treated with: (a) control treatment, (b) 1.83×10^{-1} mg/L VB, and (c) 1 mg/L VB−QDs. (B) Detection of apoptotic cells by AO/EB Staining. (Panels c, d) control cell nuclei, apoptotic nuclei from HepG2/ADM cells are observed. (Panels a, b) apoptotic nuclei could be identified by their distinctively marginated and fragmented appearance under fluorescence microscope. Bar: 10 μm. (C) SEM images of HepG2/ADM cells. (a) The cells without treatment, (b) HepG2/ADM cells after incubation with 1 mg/L VB−QDs for 1 h. Bar: 10 μm. (D) Western blotting *in vitro*. Cell lysates were prepared from the cells treated with (b) 1.83×10^{-1} mg/L VB, (c) 1 mg/L VB−QDs. HepG2/ADM cells without treatment were used as a (a) control. The antibodies were used: anti-cleaved Caspase 3 antibody. E: HepG2/ADM cells were treated with (1) control cells without any treatment, (2) 1.83×10^{-1} mg/L VB, or (3) 1 mg/L VB−QDs, quantitative analysis of apoptotic cells after various treatments, $^* p < 0.05$, compared to the control treatment (color online).

fragmentations were also examined, and cancer cell without treatment was chosen as the negative control. As seen in Fig. 3(A), VB−QDs treatment showed a high degree of the intensity of fragmented chromosomal DNA bands after 48 h treatment. Those results indicated that VB−QDs had the ability to induce cancer cells apoptosis through a process called nuclear apoptosis, which initiated DNA fragmentation and chromatin condensation. To further explore the molecular mechanisms underlying the VB−QDs-mediated apoptosis in cancer cells, we investigated apoptosis related protein expression in cancer cells. When cancer cells were treated with VB-QDs, the cleaved Caspase 3 signals on western blots were much stronger than those for cells treated with VB alone [see Fig. 3(D)].

3.3. *Morphological images of treated HepG2/ADM cells by SEM analysis*

VB−QDs lead to apparent morphological change of cancer cell, and the cancer cell membrane surface became more rough. VB−QDs caused the formation of "holes" and formed plasma membrane budding on the surface of cell membrane [see Fig. 3(C), b], compared with cancer cells untreated [see Fig. 3(C), a].

3.4. *Tumor growth inhibition study*

The nude mice were inoculated with HepG2/ADM cells and the subsequent tumor growth was recorded after various treatments. From Fig. 4(B), the HepG2/ADM nude mice, the tumor volume of the control group enlarged to almost 5090 mm^3 (group

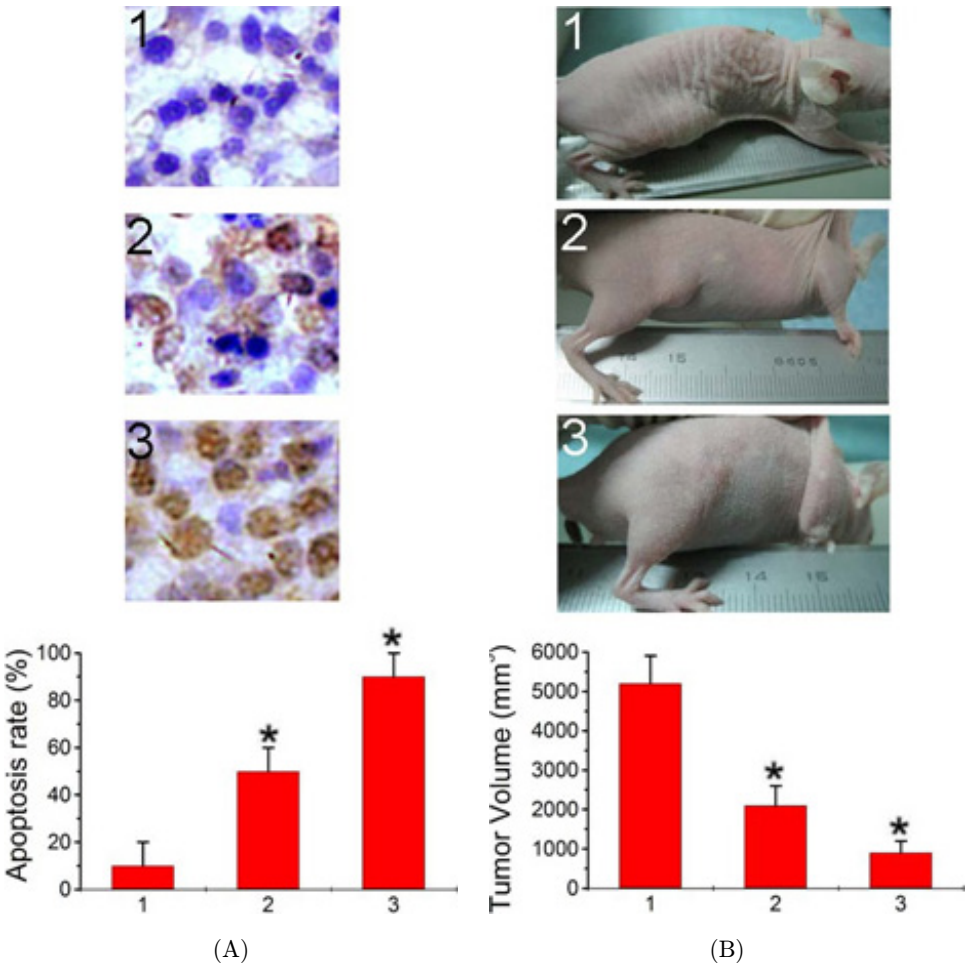

Fig. 4. (A) Immunohistochemical staining of apoptotic cells in HepG2/ADM xenograft tumors. TUNEL staining was performed on tissue sections of xenograft tumors treated as follows: group 1, untreated; group 2, 1.83×10^{-1} mg/Kg VB; group 3, 1 mg/kg VB−QDs. (B) The effect of different treatments on the tumor growth inhibition in nude mice inoculated with cancer cells. Group 1, no treatment; group 2, 1.83×10^{-1} mg/kg VB; group 3, 1mg/kg VB−QDs; $^*p < 0.05$, compared to the control treatment (color online).

1). Treatment with VB alone had mild inhibitory effect on the tumor growth in the HepG2/ADM mice due to multidrug resistance of the HepG2/ADM cell system (groups 2). However, in the group treated with VB−QDs (group 3), tumor growth was significantly inhibited.

3.5. *Analysis of cell apoptosis in HepG2/ADM xenograft tumors*

The synergistic effect of VB−QDs on the apoptosis induction in the xenograft tumors excised from nude mice, and the apoptotic rate in the control group was around 8.9% [see Fig. 4(A)]. VB−QDs treatment causes a striking increase in the number of TUNEL-positive nuclei 89.3%, compared to VB treatment 48.2%. The result of apoptosis rate was well correlated with the result of tumor growth inhibition in the studied animals.

4. Discussion

More recently, QDs had been reported to inhibit tumor angiogenesis and tumor growth, as well as promoting apoptosis, which is considered as a cancer suppressor.[5,8] In addition, our previous results had shown that QDs had potential clinical reagents applicable drug delivery *in vitro* and *in vivo*.[5] VB was one kind of water-insoluble anti-cancer drug, which has been clinically used for many years in traditional Chinese medicine (TCM).[9] We demonstrated that a combination of QDs and VB, where the VB was bound on the QDs surface by covalent bonding by FT-IR spectroscopy. The average size of VB−QDs is 6 nm, which could enhance the delivery and treatment efficiency of anti-cancer drugs.

HPLC provided quality assessment of the VB−QDs. Our current results showed that the concentration of VB was significantly high in VB−QDs. The ability to activate the apoptotic program is a mechanism for anti-cancer drugs to destroy tumor cells.[10] In this study, our results show that VB−QDs efficiently inhibited cancer cell lines growth and induced apoptosis. After AO/EB staining, the cancer cells exposed to VB−QDs revealed marked nuclear condensation, nuclear fragmentation and apoptotic bodies in Fig. 3(B). The green apoptotic nuclei are early apoptotic nuclei, and the red apoptotic nuclei are late apoptotic nuclei. However, the control group did not display any of the apoptosis characteristics. The results presented in Fig. 3(E) showed that VB−QDs indicated the increase in cell apoptosis. Furthermore, VB−QDs attenuated nuclear chromatin were condensed and DNA fragmentation accompanied with the morphological appearance of apoptosis were obtained together, resulting in cell death. The downstream effector caspases, such as Caspases 3, thus lead to DNA fragmentation and cell death.[11,12] We found that VB−QDs treatments increased cleaved Caspases 3 expression to induce apoptosis in cancer cells. Cleaved Caspases 3 facilitate process of DNA fragmentation correlated with mentioned result in Fig. 3(D).

SEM studies indicated that all the VB−QDs readily lead to apparent morphological defects change of tumor cell. By the contrast, HepG2/ADM cells untreated do not show membrane defects. This may be the reason why membrane permeability showed the most dramatic increase. Taken together, these data were consistent with the hypothesis that VB−QDs induced the formation of nanoscale holes in living cells and that these holes may allow a greatly enhanced delivery of anticancer across the cell membrane in Fig. 3(C).

A successful anti-cancer treatment should have the capability to efficiently inhibit cancer cell growth *in vivo*. As shown in our data, VB was unable to significantly inhibit the tumor growth in HepG2/ADM mice due to the multidrug resistance of this cell line. However, VB−QDs in HepG2/ADM mice greatly enhanced anti-tumor activity, suggesting the synergetic effect of QDs with VB in Fig. 4(B). Consequently, as shown in Fig. 4(A), TUNEL results demonstrated that tumor growth was inhibited by apoptosis effect of VB−QDs *in vivo*. The *in vitro* and *in vivo* results of the current study further supported suggesting the crucial role of the VB−QDs to induce cancer cell apoptosis.

5. Conclusion

This works demonstrated the utility of easy process for the synthesis of VB−QDs for inducing cancer cellular apoptosis. Based on dye staining, DNA fragmentation and Western blots assay, it was evident that VB−QDs could effectively induce cancer cellular apoptosis. SEM showed that VB−QDs could cause the "hole" formation and also lead to apparent morphological defects change of tumor cells. Results suggested that VB−QDs could be a candidate as a promising chemotherapeutic agent

in vivo, especially for treatment of the drug-resistant cancer.

Acknowledgment

This research was financially supported by QingHai science and Technology Department Youth Fund 2012-Z-920Q, NSFC 31201003, Priority Academic Program Development of Jiangsu Higher Education Institutions, and Nanjing Medical University Science and Technology Development Fund 2012NJMU022, Science and technology innovation supporting fund.

References

1. I. Brigger, C. Dubernet and P. Couvreur, *Adv. Drug Deliv. Rev.* **54**, 631 (2002).
2. G. Zhang, B. B. Lai, Y. Y. Zhou, B. A. Chen, X. M. Wang, Q. Lu and Y. Chen, *Nanomedicine: NBM.* **7**, 595 (2011).
3. M. Deepak and S. S. Handa, *Phytother. Res.* **14**, 463 (2000).
4. G. Zhang, L. Ding, R. Renegar, X. M. Wang, Q. Lu, S. Huo and Y. Chen, *J. Cancer Sci.* **102**, 1216 (2011).
5. G. Zhang, L. Shi, M. Selke and X. Wang, *Nanoscale Res. Lett.* **6**, 418 (2011).
6. S. Y. Shi, H. H. Zhou, Y. P. Zhang, X, Y. Jiang, X. Q. Chen and K. L. Huang, *Trends Anal. Chem.* **28**, 965 (2009).
7. Y. A. G-Aguirre, A. Zamilpa and M. G-Cortazar, *Ind. Crops Prod.* **36**, 188 (2012).
8. D. Shao, Q. Zeng, Z. Fan, J. Li, M. Zhang, Y. Zhang, O. Li, L. Chen, X. Kong and H. Zhang, *Biomaterials* **33**, 4336 (2012).
9. H. Zhou, Q. Yan, B. Z. Lin, Y. F. Wang and R. C. Chen, *Cancer* **16**, 29 (1997).
10. Y. R. Fu, Z. J. Yi, Y. R. Yan and Z. Y. Qiu, *Mitochondrion* **6**, 211 (2006).
11. G. Iannolo, C. Conticello, L. Memeoa and R. De Maria, *Oncology/Hematology* **66**, 42 (2008).
12. G. Zhang, H. Jiang and X. M. Wang, *NANO* **6**, 589 (2011).